Effect of Pyridoxal Phosphate and L-Ser Bound on Human Serine Hydroxymethyltransferase By Molecular Dynamics Simulations

Peerapong Wongpituk[1], Pitchayathida Mee-udorn[2], Supot Hannongbua[3,*] and Thanyada Rungrotmongkol [2,4,*]

[1]Department of Chemistry, Faculty of Science, Chulalongkorn University, Bangkok, Thailand

[2]Department of Bioinformatics and Computational Biology, Graduate School, Chulalongkorn University, Bangkok, Thailand

[3]Chemistry, Faculty of Science, Chulalongkorn University, Bangkok, Thailand

[4]Department of Biochemistry, Faculty of Science, Chulalongkorn University, Bangkok, Thailand

[*]E-mail: Thanyada.r@Chula.ac.th; Fax: +66-2218- 5418; Tel. +66-2218- 5426

ABSTRACT

Serine hydroxymethyltransferase (SHMT), a pyridoxal phosphate (PLP)-dependent enzyme, is involved in one-carbon metabolism. This enzyme catalyzes L-serine and tetrahydrofolate (THF) to glycine and 5,10-methylenetetrahydrofolate (5,10-CH_2-THF). In this study, molecular dynamics simulation was applied on wild-type human cytosolic SHMT (hcSHMT) tetramer in complex with PLP-Lys and L-ser in order to understand its structure and dynamics properties. The results, 1D- and 2D-RMSD plots versus simulation time of 100 ns suggest that the system reached the equilibrium at 30 ns, and thus the snapshots from the last 20 ns were extracted for analysis. The B-factor showed high stability of the whole tetramer in particular at the active site. The average per-residue decomposition free energy results showed the five key residues (S53, H148, S203, PLP-lys and R402) interacted with L-ser. Particularly, R402 had the strongest binding affinity (-10.09 kcal mol^{-1}) with L-ser. Additionally, the hydrogen bonding calculation provides residues of S53, S203, and K257 which indicates a strong H-bond with L-ser. PLP-lys (87%) had the strongest percentage of hydrogen bond. Thus, PLP-lys enzyme that catalyzes the reversible transfer of a carbon-unit from the L-serine to a second co-factor, the tetrahydrofolate (THF). The water accessibility at the active pocket observed by SASA calculation was around 68.25±18.83 $Å^2$. These effects of wild-type hcSHMT with PLP-lys and L-ser bound can be used as the supporting evidence to understand the structure and dynamics of wild-type hcSHMT, which can now be used to develop inhibitors targeting SHMT and, therefore, antimalarial drugs.

Keywords: Serine hydroxymethyltransferase, Molecular dynamics simulations, pyridoxal phosphate, L-serine

1. Introduction

Serine hydroxymethyltransferase (SHMT, EC 2.1.2.1.) is a pyridoxal phosphate (PLP)-dependent enzyme that is involved in one-carbon metabolism. This enzyme catalyzes L-serine and tetrahydrofolate (THF) to glycine

and 5,10-methylenetetrahydrofolate (5,10-CH_2-THF). It provides activated one-carbon units for the synthesis of dTMP, choline and amino acids [1]. The 5,10-CH_2-THF serves as a methyl donor for the thymidylate synthase (TS) reaction to convert dUMP to dTMP which is a requisite precursor for DNA or RNA biosynthesis [2]. Due to its important role in DNA or RNA biosynthesis, cell proliferation and cell survival, SHMT is one of the attractive targets for antimalarial drug discovery and development [3, 4, 5, 6, 7, 8, 9, 10] and anticancer chemotherapy [8, 11, 12, 13]. At present, structural coordinates for SHMT are available from nine organisms. Most of them are internal aldimines with a catalytic lysine residue linked to PLP or external aldimines with PLP linked to L-serine (L-ser) or L-glycine. The first step of the mechanism would be valuable for provide a suitable foundation in the design of hcSHMT inhibitors, which could be used for developing of c.

Although SHMT has gathered attention in the last two years, this enzyme continues to be poorly understood. It requires the participation of two co-factors (PLP and THF). The multisequential steps are involved in the cyclization of the THF into the final product, 5,10-CH_2-THF. This fact is very important as it provides insight into the enzymatic activity. The information on the molecular level can then be used for developing new antimalarial inhibitors towards SHMT.

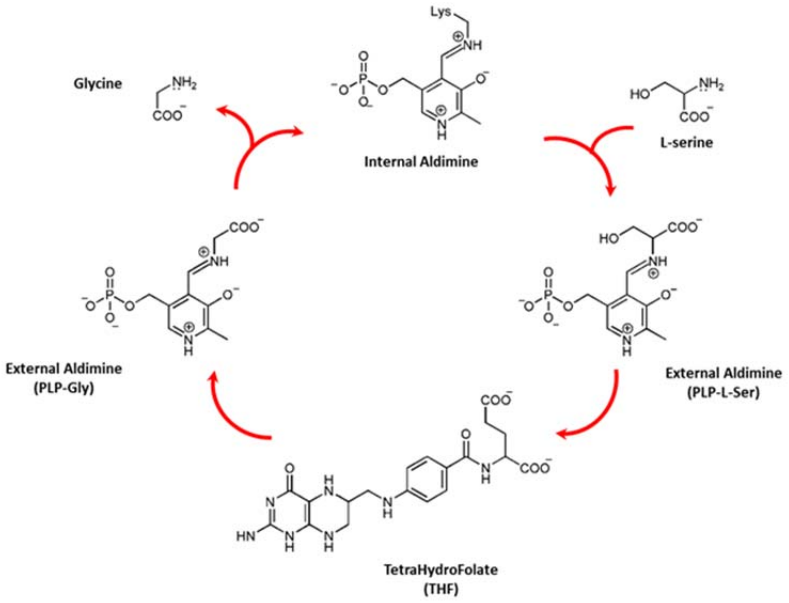

Figure 1. Scheme representing the mechanism behind the internal and external aldimine formation for PLP-dependent enzymes and the specific α- elimination reaction.

The catalytic activity of this enzyme is composed of three stages. The first two stages are common to all PLP-dependent enzymes and were already studied [14, 15]. The first stage involves the activation of the enzyme, in which the PLP cofactor becomes covalently bonded to an active site Lys residue, commonly known as the internal aldimine (PLP-lys). The second stage is triggered when the substrate is available, and it becomes covalently bonded

to the PLP cofactor, forming the external aldimine (PLP-ser or PLP-Gly). The third stage is what differentiates the PLP-dependent enzymes, and it is specific to each class of enzymes. In the case of SHMT, the enzyme catalyzes an α-elimination of L-ser that is subsequently inserted into the THF cofactor. The crystal structures of human cytosolic were successfully solved at 2.65 Å (PDB code 1BJ4) [15]. For hcSHMT, its physiological roles in nucleotide biosynthesis and involvement in cancer proliferation have been reported. Its expression level is increased rapidly during cell division, especially in cancer cells.

In the present study, molecular dynamics (MD) simulation was performed on the hcSHMT homotetramer with a presence of PLP-lys and L-ser (Figure 2). A better understanding of the structure and mechanism of SHMT would be valuable for the development and discovery of better inhibitors or agents to decrease SHMT activity which may be promising candidates for antimalarial drugs.

2. Objectives of the study

To study the effect of wild-type hcSHMT with PLP-L-ser bound in terms of structural stability, molecular dynamics behavior and binding affinities.

3. Materials and methods

Initial structure and system preparation

The tetrametic structure of human cytosolic SHMT (hcSHMT) was built by SAXS-derived molecular envelope, which was generated by superimposing the available crystal structure (PDB code 1BJ4) as a template to construct the tetrameric SHMT model as done in our previous study [19]. The starting configurations of SHMT with PLP covalently bound to Lys247 were taken from our previous study [19]. The protonation states of all ionizable amino acids (D, E, K, R, and H) were assigned at physiological pH 7.0 using PDB2PQR Version 2.0.0 [20]. To obtain the complexes between hcSHMT, L-serine, and PLP cofactor the structure of L-ser was superimposed with crystal structure in the Protein Data Bank (PDB code 1BJ4) and (PDB code 1DFO) using Chimera software [20]. The geometric optimization of PLP was performed at the HF/6-31(d) level of theory using Gaussian09 software [21]. The atomic charges of PLP were developed according to standard procedure [22]. The AMBER ff14SB force field [23] was adopted for the protein and also for L-ser as ligand, while the atom types and the other molecular parameters of PLP were assigned by generic AMBER force field version 2 (GAFF2) [23]. Additionally the electrostatic potential (ESP) charges of each ligand were calculated with the same method. Subsequently, the restrained ESP (RESP) charges conversion was carried out from the ESP charges using the ANTECHAMBER module in the AMBER package. The missing hydrogen atoms were added using Leap module of the AMBER16 software [24]. Following, the added hydrogen atoms were minimized with 2500 steps of steepest descents (SD) followed by 2500 steps of conjugated gradient (CG). Afterwards, the hcSHMT complex was solvated by TIP3P water model of 32,887 water molecules in octahedral box within 10 Å from the protein surface. The

water molecules were then minimized with 1000 steps of SD algorithm and continued by 2500 steps of CG algorithm. The total charges with negative value of the complexes were randomly neutralized by adding 16 Na+ ions. The whole system was fully minimized using the aforementioned minimization process. All covalent bonds involving hydrogen atoms were constrained using SHAKE algorithm. [25]

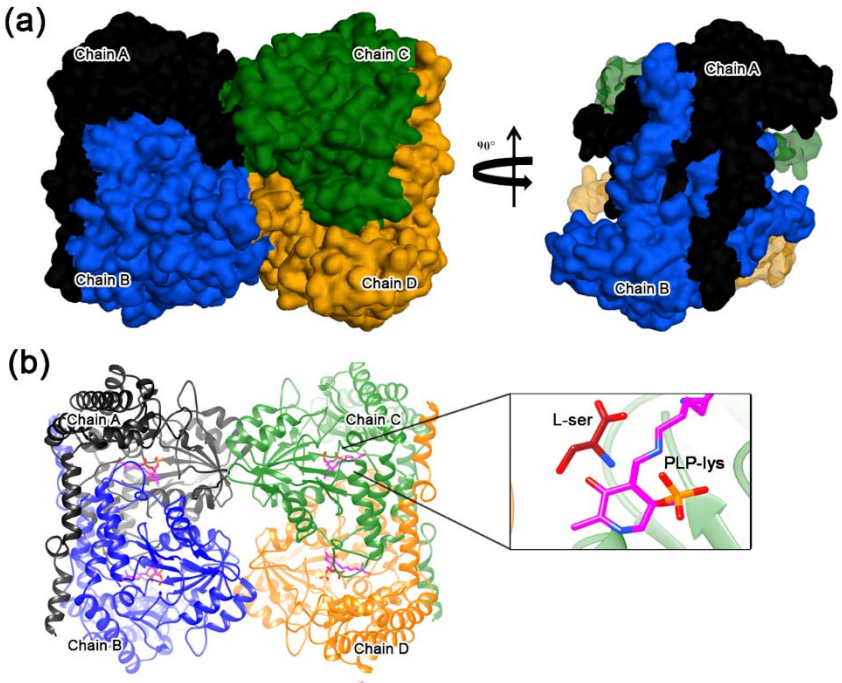

Figure 2. Structure of tetrameric hcSHMT (a) Surface representation showing vast inter-subunit interfaces within tight, vertically arranged dimers and contacts between the two dimers, where the secondary structure elements with the locations of PLP covalent bound with K257 (PLP-Lys) and L-ser are given in (b).

Molecular dynamics simulation

Molecular dynamics (MD) simulation was used to study the structure and dynamic properties of hcSHMT/L-ser. For this study, the system surrounded by the periodic boundary condition with NPT ensemble and a simulation time step of 2 fs time step were used. The system was heated from 10 K to 298 K for 100 ps. The simulation was then run at this temperature and a pressure of 1 atm for 50 ns using the PMEMD module in AMBER16 program. To indicate the system stability, the root mean square displacement (RMSD) and the B-factor were analyzed using the CPPTRAJ module with the built-in function of AMBER16. Meanwhile, the ligand-protein interaction was calculated with the per-residue decomposition of MM-GBSA binding free energy ($\Delta G_{bind}^{residue}$). Other structural analyses, including the average hydrogen bond formation, solvent accessible surface area (SASA), number of contact residue and solvated interaction energy were also calculated by the CPPTRAJ module.

4. Results

System stability of simulated models

The stability of each simulated chain of wild-type hcSHMT was determined by root mean square displacement (RMSD) and two dimension RMSD (2D-RMSD) calculations relative to the starting structure along the 100 ns simulation. The RMSD values of four chain complexes maintain at a fluctuation of around 1.35 to 2.26 Å until the end of simulation time as shown in Figure 3(a). The RMSD results suggest that simulated systems have reached equilibrium at 100 ns, and thus the snapshots taken from the last 20 ns of the simulation are selected for further analysis. Moreover, the four chains of wild-type hcSHMT provide relatively similar 2D-RMSD patterns of the complexes as shown in Figure 3(b).

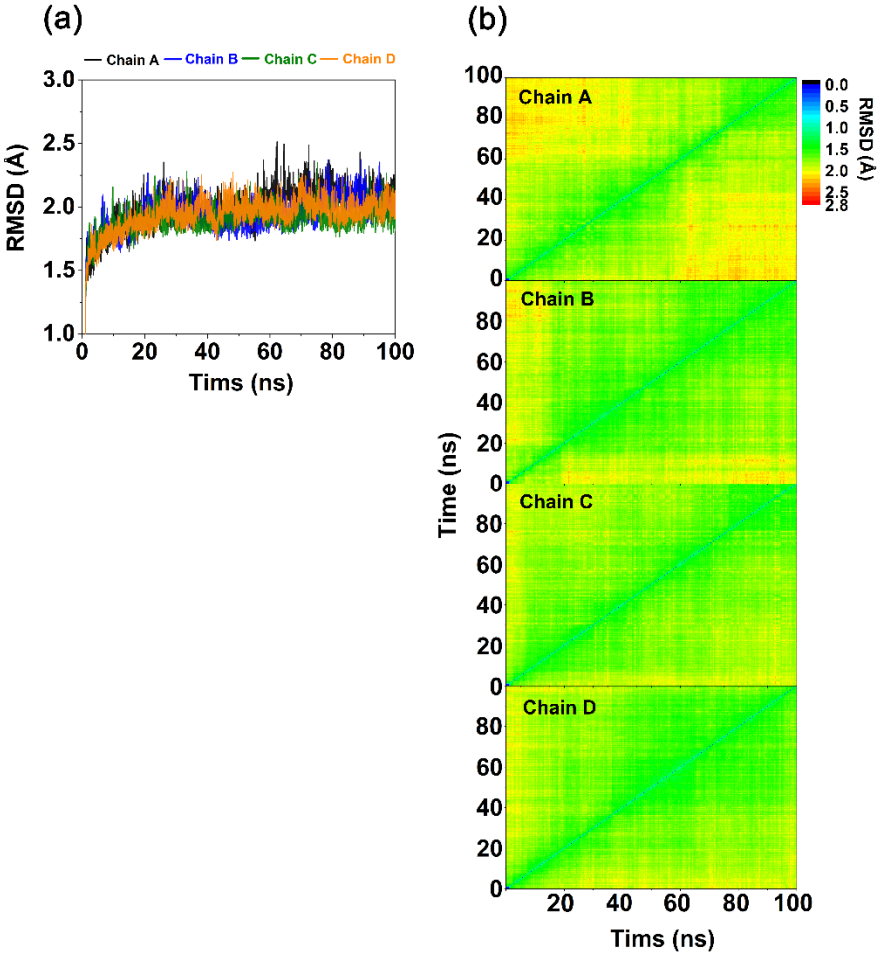

Figure 3. RMSD (a) and 2D-RMSD (b) plots for all atoms of chain A (black), chain B (blue), chain C (green) and chain D (orange) of wild-type hcSHMT with PLP-lys and L-ser bound.

B-factor

To assess protein mobility and dynamics of wild-type hcSHMT, the structures were subjected to last 20 ns MD simulations. The output of the simulation show the relationship between structural integrity and the B-factor, which indicates thermal motion of the molecules. The results demonstrate that the protein structure of wild-type hcSHMT with L-ser form is rigid at the binding pocket and the whole structure is quite stable as shown in Figure 4. This suggests that wild-type hcSHMT with PLP-lys and L-ser bound is not a functional structure of this enzyme. Therefore, the binding pocket is highly stable. However, some enzyme parts that solvate in the water are quite flexible along the MD simulation [26].

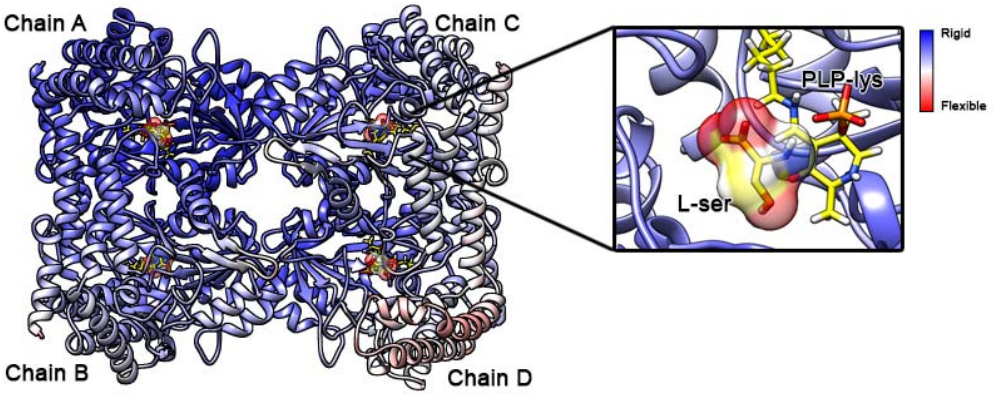

Figure 4. Normalized B-factor at last 20 ns MD simulation of wild-type hcSHMT with PLP-lys and L-ser bound.

Distances between C7 atom of PLP-lys and N atom of L-ser

To determine the occurrence of external aldimine (PLP bound with L-ser) the distance between C7 atom of PLP (covalently bound with K257) and N atom of L-ser along the simulation was measured. The result shows that distances between C7 atom of PLP-lys and N atom of L-ser are stable. Meanwhile, the distributions of distances show peaks around 4 to 10 Å (Figure 5.). This result suggests that the distances between the C7 atom of PLP-lys and N atom of L-ser are in the position that might form the external aldimine.

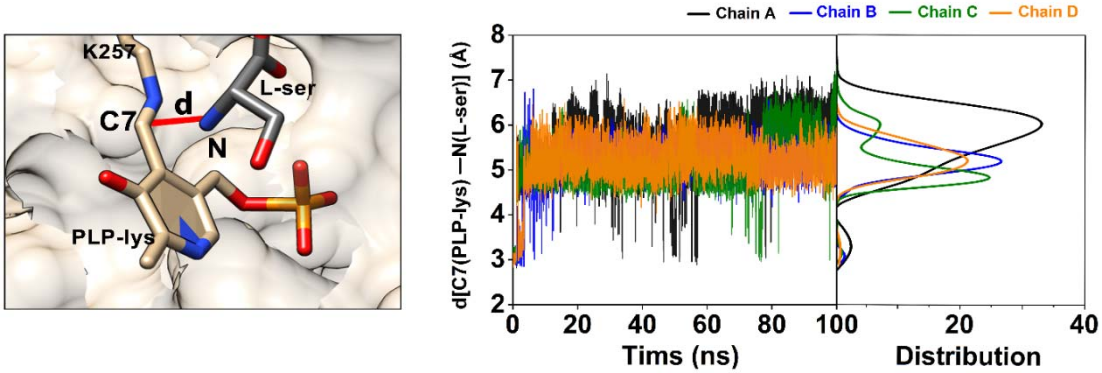

Figure 5. Distances between the C7 atoms of PLP-lys and N atom of L-ser in chain A (black), chain B (blue), chain C (green) and chain D (orange) for wild-type hcSHMT.

Intermolecular interactions of protein-ligand interface

The per-residue decomposition free energy ($\Delta G_{bind}^{residue}$) calculation based on the molecular mechanics/generalized born surface area (MM-GBSA) method was performed at last 20 ns in order to evaluate the key residues of wild-type hcSHMT involved in L-ser bound. The average contribution of each amino acid for L-ser of all chain complexes are plotted in Figure 6. Only the residues which show the energy contribution less than -1.0 kcal/mol or higher than 1.0 kcal/mol are considered and plotted. The negative and positive decomposition free energy values represent the structural stabilization and destabilization, respectively. In the case of wild-type hcSHMT with PLP-lys and L-ser bound, there are five key residues (S53, H148, S203, PLP-lys and R402) playing a role as important residues for stabilizing the active site of the enzyme with L-ser bound. The results show that R402 residue had the strongest binding affinity toward PLP binding ($\Delta G_{bind}^{residue}$ of -10.09 kcal mol^{-1}, red) because of the salt bridge effect between phosphate group of PLP-lys and side chain of R402.

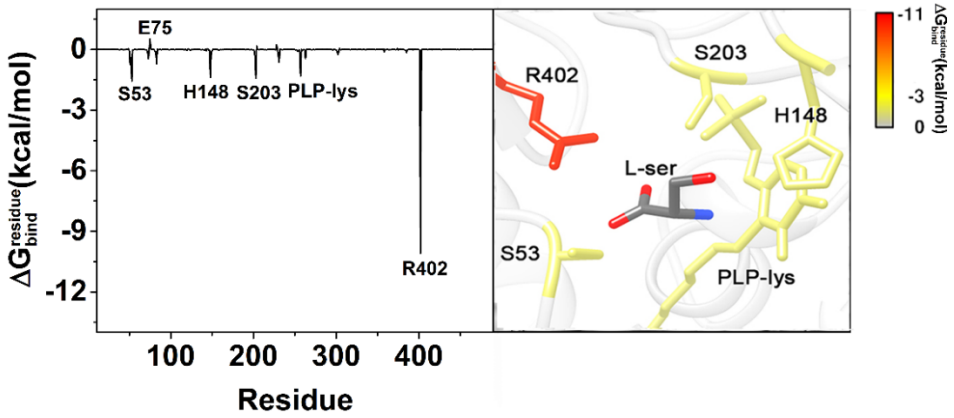

Figure 6. The average value of per-residue energy (kcal mol-1) of wild-type hcSHMT structure with PLP-lys and L-ser bound. The important amino acids for ligand binding are shaded based on their decomposition energy, where the highest and lowest energies are ranging from gray to red, respectively.

The hydrogen bond (H-bond) formation is one of the important factors that can determine the binding strength of ligand-protein interactions. The intermolecular hydrogen bonds were calculated using the two criteria: (i) distance between hydrogen donor (HD) and hydrogen acceptor (HA) $\leq$ 3.5 Å, and (ii) the angle of HD - H$\cdots$HA $\geq$ 120°. The hydrogen bond strengths are divided into 3 levels: low (10–39%), moderate (40–69%), and strong (70–100%) interactions represented by the gradient of greenish, bluish and reddish grid cells, respectively (Figure 7.). It shows the average percentage of H-bond at the last 20 ns for the four chains of wild-type hcSHMT. A similar H-bond pattern across ligand-protein interface is found in complexes with a strong interaction between the backbone atoms of L-ser and hcSHMT. The results indicate strong occupation ranging from 71 to 100%, as illustrated in Figure 7 with the numbers of reddish cells of S53(79%), S203(82%) and PLP-lys(87%). These intermolecular hydrogen bonds support the ligand binding to wild-type hcSHMT, but it is not the main force for ligand-protein complexation as discussed above in term of molecular mechanics energy.

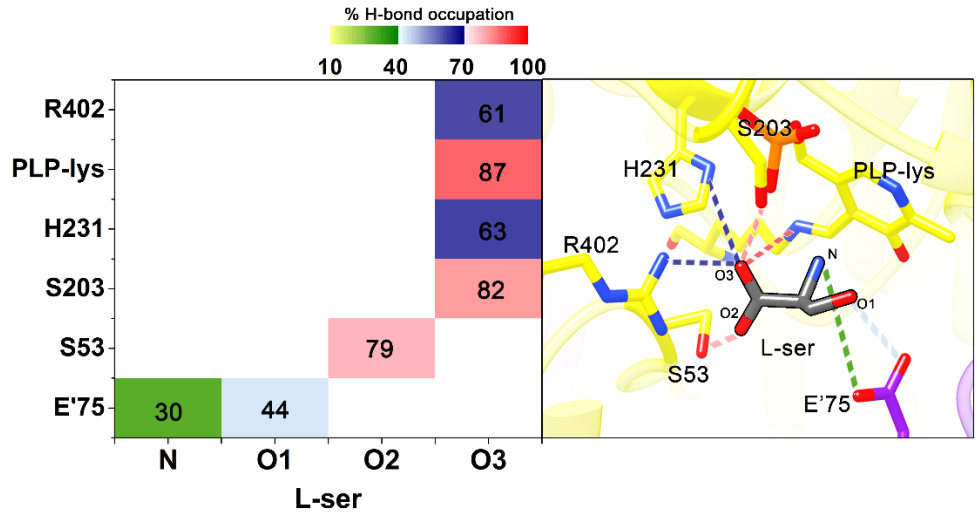

Figure 7. The average percentage of hydrogen bond occupation between L-ser and hcSHMT in four chain complexes. (a) The structure of H-bond interactions between L-ser and hcSHMT (b) at last 20 ns.

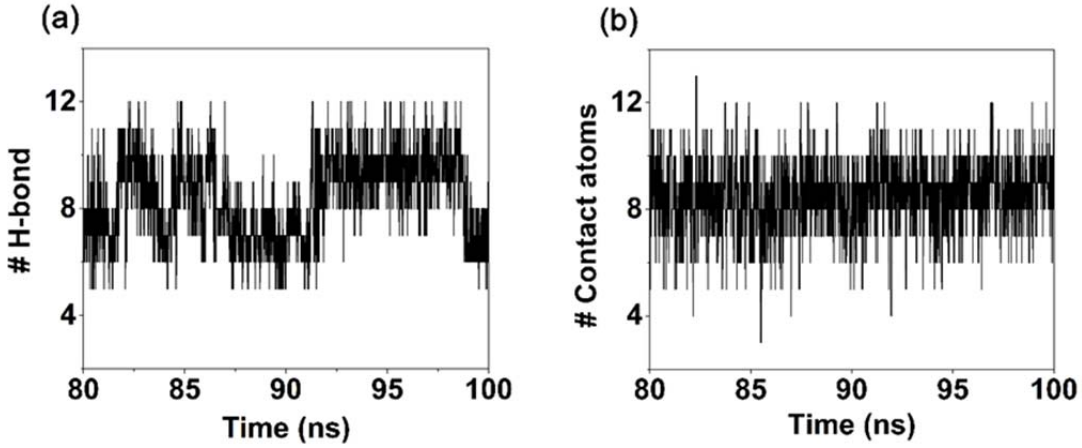

Figure 8. Average number of H-bond between hcSHMT with L-ser bound (a). Average number of contact atoms between the binding pocket of tetrameric wild-type hcSHMT with L-ser bound within 5.0 Å cutoff at last 20 ns (b).

The average number of contact atoms and the average number of H-bond at the binding pocket around the ligands point to hcSHMT which bonded PLP with L-ser bound had on average 8 contact atoms Figure 8(b) and average number of H-bond had on average around 8 bonds Figure 8(a). This indicates that the contact atoms and H-bond between hcSHMT with L-ser has been found from the beginning until the end of MD simulations, suggesting that L-ser which bonded hcSHMT is stable in the binding pocket of wild-type hcSHMT.

Solvent accessibility at the hcSHMT binding pocket

Solvent accessible surface area (SASA) is the surface area of solvent molecules that can access to a binding pocket, which might play an important role for ligand binding to proteins. To study the effect of solvent accessibility on the wild-type hcSHMT binding pocket, the SASA calculation on L-ser as well as 5 Å sphere of L-ser was performed in Figure 9(b) (i.e., 139-141, 192-194, 218, 220-245, 247-251, 287, 291-293, 392, 396). The

results are summarized and compared to Figure 9. The average SASA value over the last 20 ns of wild-type hcSHMT binding pocket was 68.25±18.83 $Å^2$. As a result from this method it can be concluded that L-ser has quite low of SASA value which mean L-ser has good binding affinity with hcSHMT shown by the close interaction with hcSHMT binding pocket.

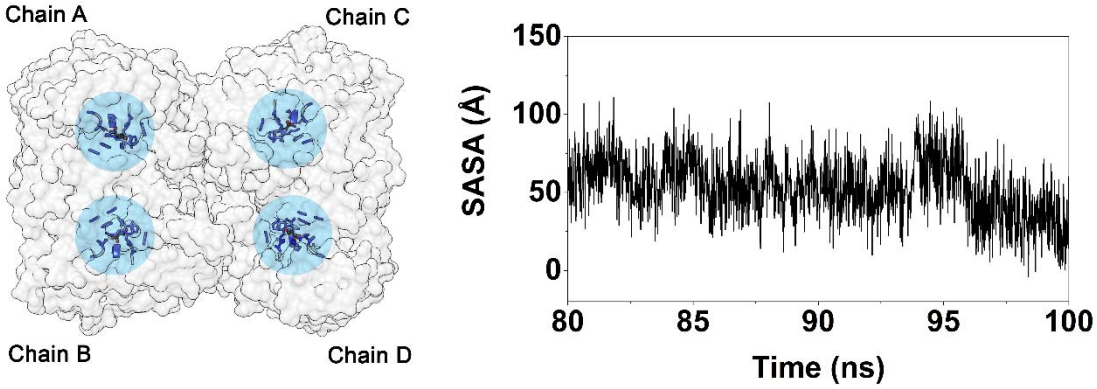

Figure 9.The average solvent accessible surface area (SASA) within a 5Å sphere of L-ser bound with wild-type hcSHMT in four chains and the area of calculation for solvent accessible surface area.

5. Discussion

In the present study of tetrameric wild-type hcSHMT using Molecular dynamics simulation we show the protein stability and dynamics at the binding pocket and at the entire system. In this work we focus on the first step of mechanism in which PLP-dependent enzyme with L-ser bond catalyze the reversible transfer of one carbon from L-ser to tetrahydrofolate (THF) (see Figure 1) in the way through which the hydroxymethyl group is transferred from L-serine. At the end of the reaction, a glycine is released.

Analytical techniques including RMSD, 2D-RMSD, B-factor, the number of H-bond and the number of contact atom are showing the stability of tetrameric wild-type hcSHMT, The results of RMSD along the 100 ns indicate that the systems reached the equilibrium at ~80 ns as well as 2D-RMSD are showing a green area at last 20 ns, which means the system of tetrameric wild-type hcSHMT is stable. These results are also supported by the number of contact atoms, the number of H-bond and B-factors because the number of contact atoms between L-ser with hcSHMT are showing the number of contact atoms around 8 atoms from the beginning of last 80 ns until 100 ns which indicates that the binding pocket of wild-type hcSHMT is stable as well as the number of H-bond is stable during the last 20 ns. Likewise, the B-factor of the protein was quite stable along the 20 ns simulation that supports equilibrium times at least 20 ns.

According to intermolecular interactions of L-ser, residues of PLP-lys, S53, and S203 show strong H-bond with L-ser respectively; PLP-lys (87%) had the strongest percentage of hydrogen bond with C7 of PLP-lys which is the position that form the external aldimin. Thus, PLP-lys enzyme catalyzes the reversible transfer of a carbon-unit from the L-serine to a second cofactor, the tetrahydrofolate (THF) (see Figure 1). Similar to per-residue

decomposition free energy analysis, PLP-lys are showing strong binding affinity with L-ser ($\Delta G_{bind}^{residue}$ of -1.31 kcal mol^{-1}). These result support the mechanism which first step is L-ser bonding to PLP (external aldimine).

The result of per-residue decomposition free energy analysis has found four residues of wild-type hcSHMT (S53, H148, S203, and R402) which play a role as important residues for stabilizing the active site with L-ser bound. Moreover, the average per-residue decomposition free energy result show that the R402 has the strongest binding affinity ($\Delta G_{bind}^{residue}$ of -10.09 kcal mol^{-1}) with L-ser due to the salt-bridge interaction effect between the R402 side chain and the carboxyl group of L-Ser [17]. In particular, solvent accessible surface area (SASA) is supporting that L-ser has good binding affinity with hcSHMT shown by the close interaction with hcSHMT binding pocket.

E'75 was found to play a key role in the result of per-residue decomposition free energy analysis ($\Delta G_{bind}^{residue}$ of 1.51 kcal mol^{-1}) and H-bond. This is consistent with the mutagenic studies that show that any mutations to Glu75 caused a drastic inhibitor of enzyme [27-29]. Additionally, Glu75 works as a proton pump that handles the charge transfers across the mechanism and establishes a link between the external aldimine and the THF cofactor [30].

6. Conclusion

Our current study of tetrameric wild-type hcSHMT has shown for the first time that interaction between L-ser with hcSHMT and the key in stabilization of tetrameric structures. The structures of the molecules described in this report provide a better understanding of the structure and mechanism of SHMT, which is valuable for establishing a suitable foundation in the design of hcSHMT inhibitors, which could be used for the development of anticancer drugs.

Acknowledgement

We would like to thank the Center of Excellent in Computational Chemistry for providing us the facilities and computing resources. We would like to thank Dr. Penchit Chitnumsub and Dr. Somchart Maenpuen for providing the research topic and for helpful discussions. Additionally, we would like to thank Faculty of Science, Chulalongkorn University and Thailand Research Fund (IRG5780008) and all members of Biosimulation laboratory, Department of Biochemistry, Faculty of Science, Chulalongkorn University.

References

[1] Muller, I. B. and Hyde, J. E., Mol. Biochem. Parasitol., 2013, 188, 63–77.

[2] Alfadhli, S., and Rathod, P. K., Mol. Biochem. Parasitol, 2000, 110, 283-291.

[3] Nirmalan, N., Wang, P., Sims, P. F., and Hyde, J. E., Mol Microbiol, 2002, 46, 179-190.

[4] Leartsakulpanich, U., Kongkasuriyachai, D., Imwong, M., Chotivanich, K., and Yuthavong, Y., Parasitol. Int., 2008. 57, 223-228.

[5] Maenpuen, S., Sopitthummakhun, K., Yuthavong, Y., Chaiyen, P., and Leartsakulpanich, U., Mol. Biochem Parasitol, 2009, 168, 63-73.

[6] Pornthanakasem, W., Kongkasuriyachai, D., Uthaipibull, C., Yuthavong, Y., and Leartsakulpanich, U., Malar. J, 2012. 11, 387-395.

[7] Witschel, M. C., Rottmann, M., Schwab, A., Leartsakulpanich, U., Chitnumsub, P., Seet, M., Tonazzi, S., Schwertz, G., Stelzer, F., Mietzner, T., McNamara, C., Thater, F., Freymond, C., Jaruwat, A., Pinthong, C., Riangrungroj, P., Oufir, M., Hamburger, M., Mäser, P., Sanz-Alonso, L. M., Charman, S., Wittlin, S., Yuthavong, Y., Chaiyen, P., and Diederich, F., J. Med. Chem., 2015, 58, 3117-3130.

[8] Amornwatcharapong, W., Maenpuen, S., Chitnumsub, P., Leartsakulpanich, U., and Chaiyen, P. Arch. Biochem. Biophys., 2017, 630, 91-100.

[9] Schwertz, G., Witschel, M. C., Rottmann, M., Bonnert, R., Leartsakulpanich, U., Chitnumsub, P., Jaruwat, A., Ittarat, W., Schäfer, A., Aponte, R. A., Charman, S. A., White, K. L., Kundu, A., Sadhukhan, S., Lloyd, M., Freiberg, G. M., Srikumaran, M., Siggel, M., Zwyssig, A., Chaiyen, P., and Diederich, F. J. Med. Chem., 2017, 60, 4840-4860.

[10] Schwertz, G., Frei, M. S., Witschel, M. C., Rottmann, M., Leartsakulpanich, U., Chitnumsub, P., Jaruwat, A., Ittarat, W., Schäfer, A., Aponte, R. A., Trapp, N., Mark, K., Chaiyen, P., and Diederich, F., Chem.Euro.J., 2017, 23, 14345-14357.

[11] Paiardini, A., Fiascarelli, A., Rinaldo, S., Daidone, F., Giardina, G., Koes, D. R., Parroni, A., Montini, G., Marani, M., Paone, A., McDermott, L. A., Contestabile, R., and Cutruzzolà, F., Chem. Med. Chem., 2015, 10, 490-497.

[12] Marani, M., Paone, A., Fiascarelli, A., Macone, A., Gargano, M., Rinaldo, S., Giardina, G., Pontecorvi, V., Koes, D., McDermott, L., Yang, T., Paiardini, A., Contestabile, R., and Cutruzzolà, F., Oncotarget, 2016, 7, 4570-4583.

[13] Ducker, G. S., Ghergurovich, J. M., Mainolfi, N., Suri, V., Jeong, S. K., Hsin-Jung Li, S., Friedman, A., Manfredi, M. G., Gitai, Z., Kim, H., and Rabinowitz, J. D., Proc. Natl. Acad. Sci. U.S.A., 2017, 114, 11404-11409.

[14] Cerqueira, N. M., Fernandes, P. A., Ramos, M. J., J. Chem. Theory Comput., 2011, 7, 1356−68.

[15] Oliveira, E. F.; Cerqueira, N. M.; Fernandes, P. A.; Ramos, M. J., J. Am. Chem. Soc., 2011, 133, 15496−15505.

[16] Renwick, S. B., Snell, K., and Baumann, U., Structure, 1998, 6, 1105-1116.

[17] Chitnumsub, P., Ittarat, W., Jaruwat, A., Noytanom, K., Amornwatcharapong, W., Pornthanakasem, W., Chaiyen, P., Yuthavong, Y., and Leartsakulpanich, U., Acta Crystallogr. D. Biol. Crystallogr., 2014, 70, 1517-1527.

[18] Chitnumsub, P., Jaruwat, A., Riangrungroj, P., Ittarat, W., Noytanom, K., Oonanant, W., Vanichthanankul, J., Chuankhayan, P., Maenpuen, S., Chen, C. J., Chaiyen, P., Yuthavong, Y., and Leartsakulpanich, U., Acta Crystallogr. D. Biol. Crystallogr. 2014, 70, 3177-3186

[19] Scarsdale, J. N., Kazanina, G., Radaev, S., Schirch, V., and Wright, H. T., Biochemistry, 1999, 38, 8347-8358.

[20] Ubonprasert, S., Jaroensuk, J., Pornthanakasem, W., Kamonsutthipaijit, N., Wongpituk, P., Mee-udorn, p., Rungrotmongkol, T., Ketchart, O., Chitnumsub, p., Leartsakulpanich, U., Chaiyen, P., Maenpuen, S., JBC, 2018

[21] Dolinsky,T.J., Nielsen,J.E., McCammon,J.A. and Baker,N.A., Nucleic Acids Res., 2004, 32, W665–W667.

[22] Szebenyi, D. M., Liu, X., Kriksunov, I. A., Stover, P. J., and Thiel, D. J., Biochemistry, 2000, 39, 13313-13323.

[23] Wang, J., Wolf, R.M., Caldwell, J.W., Kollman, P.A., and Case, D.A., Journal of Computational Chemistry, 2004, 25, 1157-1174.

[24] Pinthong, C., Meanpuen, S., Amornwatcharaong, W., Yuthavong, Y., Leartsakulpanich, U., Chaiyen, P., FEBS J., 2014, 281, 2570–2583

[25] Jorgensen WL, Chandrasekhar J, Madura JD, Impey RW, & Klein ML. The Journal of chemical physics., 1983, 79(2): 926-935.

[26] Renwick, S. B., Snell, K., and Baumann, U., Structure, 1998, 6, 1105-16.

[27] Szebenyi, D. M.; Musayev, F. N.; di Salvo, M. L.; Safo, M. K.;Schirch, V. Biochemistry 2004, 43, 6865─76.

[28] Scarsdale, J. N.; Radaev, S.; Kazanina, G.; Schirch, V.; Wright,H. T. J. Mol. Biol. 2000, 296, 155─168.

[29] Rao, J. V.; Prakash, V.; Rao, N. A.; Savithri, H. S. Eur. J. Biochem. 2000, 267, 5967─76.

[30] Henrique S. Fernandes, Maria Joao Ramos, and Nuno M. F. S. A. Cerqueira. ACS Catal. 2018, 8, 10096─10110